Since January 2020 Elsevier has created a COVID-19 resource centre with free information in English and Mandarin on the novel coronavirus COVID-19. The COVID-19 resource centre is hosted on Elsevier Connect, the company's public news and information website.

Contents lists available at ScienceDirect

Digital Chinese Medicine

journal homepage: http://dcmhi.com.cn

Systematic Pharmacological Strategies to Explore the Regulatory Mechanism of Ma Xing Shi Gan Decoction on COVID-19

ZHANG Shi-Ying[a, b, c], LI Ling[a], ZHANG Ning[d, e], XIA Hong-Tao[b, c], LU Fang-Guo[a*], LI Wei-Qing[b, c*]

a. Hunan University of Chinese Medicine, Changsha, Hunan 410208, China

b. Department of Traditional Chinese Medicine, Shenzhen Luohu People's Hospital, Shenzhen, Guangdong 518001, China

c. Department of Traditional Chinese Medicine, The Third Affiliated Hospital of Shenzhen University, Shenzhen, Guangdong 518001, China

d. Department of Respiratory Disease, Shenzhen Luohu People's Hospital, Shenzhen, Guangdong 518001, China

e. Department of Respiratory Disease, The Third Affiliated Hospital of Shenzhen University, Shenzhen, Guangdong 518001, China

ARTICLE INFO

Article history
Received 07 Mar. 2020
Accepted 05 Apr. 2020
Available online 25 Jun. 2020

Keywords
Coronavirus disease 2019 (COVID-19)
Ma Xing Shi Gan Decoction (MXSGD)
Network pharmacology
Mechanism
ACE2 receptor

*Corresponding author: LI Wei-Qing, Professor. Research direction: study on the prevention and treatment of cardiopulmonary disease with TCM.
E-mail: 755960096@qq.com.
LU Fang-Guo, Professor. Research direction: study on the prevention and treatment of infectious diseases with TCM.
E-mail: 1925289120@qq.com.

Peer review under the responsibility of Hunan University of Chinese Medicine.

ABSTRACT

Objective To use systematic pharmacological strategies to explore the regulatory mechanisms of Ma Xing Shi Gan Decoction (MXSGD) against the coronavirus disease 2019 (COVID-19).

Methods Data on the compounds and targets of MXSGD were collected from the Traditional Chinese Medicene Systems Parmacology Database and Analysis Platform (TCMSP) and TCM Databases@Taiwan. Data on ACE2-related targets and the protein-protein interaction (PPI) were collected from the String database. The Cytoscape 3.7.2 was used to construct and analyze the networks. The DAVID platform was used for Gene Ontology (GO) and pathway enrichment analyses.

Results Data on 272 MXSGD targets and 21 SARS-CoV-2 potential targets were collected. Four networks were constructed and analyzed based on the data: (1) compound-target network of MXSGD; (2) MXSGD-SARS-CoV-2-PPI network; (3) cluster of MXSGD-SARS-CoV-2-PPI network; (4) Herb-Pathway-Target network. The core targets included AKT1, MAPK3, IL-6, TP53, VEGFA, TNF, CASP3, EGFR, EGF and MAPK1. The antiviral biological processes were inflammatory responses (inflammatory cells, inflammatory cytokines and their signaling pathways), immune responses (T cells, monocytes, B cells and other immune cells), immune factors (IFN-γ, TNF-α and so on), virus defense, humoral immunity and mucosal innate immune response. The antivirus-related signaling pathways included TNF, NOD-like receptor, FoxO, PI3K-AKT and Toll-like receptor signaling pathways.

Conclusions MXSGD can control disease progression by regulating multiple compounds and targets; it can reduce inflammation and balance immunity by regulating several

proteins that interact with ACE2 and signaling pathways closely related to disease development.

DOI: 10.1016/j.dcmed.2020.06.004
Citation: ZHANG SY, LI L, ZHANG N, et al. Systematic pharmacological strategies to explore the regulatory mechanism of Ma Xing Shi Gan Decoction on COVID-19. Digital Chinese Medicine, 2020,3(2): 96–115.

1 Introduction

The coronavirus disease 2019 (COVID-19), caused by the severe acute respiratory syndrome coronavirus 2 (SARS-CoV-2), has placed a huge burden on medical resources due to its high contagiousness, long incubation period, and the general susceptibility of the population [1]. However, the current treatment of COVID-19 is mainly palliative, and prompt and effective treatment planning at various stages of its course is challenging [2].

In 2003, traditional Chinese medicine (TCM) showed satisfactory treatment outcomes in the early stages of the SARS epidemic [3]. Since the third edition of "Diagnosis and Treatment Protocol for COVID-19" was released, TCM has been recommended for the treatment of COVID-19 [4]. The National Health Commission and the State Administration of Traditional Chinese Medicine jointly announced that TCM can reduces fever symptoms, glucocorticoid dosage, and complications and controls disease progression. In various versions of the “Diagnosis and Treatment Protocol for COVID-19” and according to the theory of TCM, COVID-19 is caused by epidemic Qi and the disease is localized within the lungs. The basic pathogenesis is “wet, heat, poison and blood stasis”. The basic prescriptions for dampness and stagnation of the lungs include Ephedra Herba (Ma Huang, 麻黄), Armeniacae Semen Amarum (Ku Xing Ren, 苦杏仁), Tsaoko Fructus (Cao Guo, 草果), Forsythiae Fructus (Lian Qiao, 连翘), Atractylodis Rhizoma (Cang Zhu, 苍术) and Glycyrrhizae Radix Et Rhizoma (Gan Cao, 甘草). The basic prescriptions for the syndrome of pathogenic toxin blockage of the lungs include Armeniacae Semen Amarum (Ku Xing Ren, 苦杏仁), Gypsum Fibrosum (Shi Gao, 石膏), Trichosanthis Fructus (Gua Lou, 瓜蒌), Rhei Radix Et Rhizoma (Da Huang, 大黄), Ephedra Herba (Ma Huang, 麻黄) and Glycyrrhizae Radix Et Rhizoma (Gan Cao, 甘草). The basic prescriptions for the syndrome of pathogenic heat congesting the lung include Ephedra Herba (Ma Huang, 麻黄), Armeniacae Semen Amarum (Ku Xing Ren, 苦杏仁), Gypsum Fibrosum (Shi Gao, 石膏), Fritillariae Thunbergii Bulbus (Zhe Bei Mu, 浙贝母) and Glycyrrhizae Radix Et Rhizoma (Gan Cao, 甘草). The basic prescriptions are mainly Ephedra Herba (Ma Huang, 麻黄), Armeniacae Semen Amarum (Ku Xing Ren, 苦杏仁), Glycyrrhizae Radix Et Rhizoma (Gan Cao, 甘草) and Gypsum Fibrosum (Shi Gao, 石膏) from Ma Xing Shi Gan Decoction (MXSGD). Meanwhile, the herbal formula Qing Fei Pai Du Decoction, which has good curative effects, is also mainly composed of MXSGD [5].

This research group has conducted in-depth research on the antiviral and immunoregulatory mechanisms of MXSGD. *In vitro* models have shown that MXSGD can directly inhibit influenza virus replication; it has better virus adsorption inhibitory and host cell-protective effects than ribavirin [6, 7]. MXSGD can also down-regulate IFN-α/β secretion and protein expression of influenza virus-infected macrophages [8]. *In vivo* animal experiments showed that MXSGD can inhibit the activation of the TLR4-MyD88-TRAF6 signaling pathway and alleviate lung injury caused by influenza A virus in infected mice [9]. In summary, MXSGD has demonstrated satisfactory effects against influenza viruses. The use of bioinformatics coupled with the establishment of large network databases and the development of pharmacological computer simulation technologies facilitate significant progress in pharmacology [10]. This is consistent with the overall system theory of TCM for treating diseases [11, 12]. We used bioinformatics to explore the pharmacological mechanisms and effectiveness of MXSGD in the treatment of COVID-19-related pneumonia and provide theoretical guidance and support for clinical use.

2 Materials and Methods

2.1 The bioactive compounds and targets of MXSGD

Using “Armeniacae Semen Amarum” “Glycyrrhizae Radix Et Rhizoma” “Ephedra Herba” “Gypsum Fibrosum” as keywords, the compounds of MXSGD were searched and collected from the TCM Database@Taiwan (http://tcm.cmu.edu.tw/zh-tw/index.php) [13] and Traditional Chinese Medicene Systems Parmacology Database and Analysis Platform(TCMSP)(http://tcmspw.com/index.php)[14]. Data on the pharmacokinetic parameters and these MXSGD targets were collected from TCMSP. Pharmacokinetic parameters included oral bioavailability (OB), Caco-2 permeability, and drug-likeness (DL). OB and Caco-2 permeability indicate

the degree of absorption of a compound into the blood after oral administration [15, 16]. DL, which refers to the similarity of a compound to a known drug, indicates the likelihood that the compound will become a drug [17]. According to the standards provided by the TCMSP database, all compounds were filtered, using OB > 30%, Caco-2 > – 0.4, and DL > 0.18 as standards, to obtain orally absorbable MXSGD compounds with pharmacological activity [14]. Finally, a total of 110 MXSGD bioactive compounds with targets were obtained. The details of each compound are shown in Table 1. The name of the collected target protein was imported into UniProtKB (http://www.uniprot.org/), and the species was limited to "Homo sapiens" to allow the corrections of the names of the proteins to their official symbols.

2.2 SARS-CoV-2 target and protein-protein interaction (PPI) data collection

The OMIM database (http://omim.org/) and Genecards (http://www.genecards.org) were used to collect data on the targets of SARS-CoV-2 [18, 19]. Meanwhile, this study would also use the String database to collect PPI data for the targets of MXSGD and SARS-CoV-2. When collecting data, the species were limited to "Homo sapiens" with a confidence level of > 0.4 [20].

2.3 Network construction and analysis methods

The MXSGD target, SARS-CoV-2 potential target, and PPI data were imported into the network visualization software, Cytoscape 3.7.2, to build and analyze the networks [21]. In the network, a node represents the active compound, target or pathway, and nodes are connected by edges. The meaning of an edge varies with networks [21]. The degree represents the number of connections between nodes, and betweenness represents the number of shortest paths through nodes [21]. In a large PPI network, there are dense areas of some molecular complexes, which are defined as clusters. In the MXSGD-SARS-CoV-2-PPI network, clusters can be considered as functional modules. It is possible to treat diseases by interacting with these functional modules [21]. The plug-in MCODE of Cytoscape 3.7.2 can analyze the PPI network to find clusters.

2.4 Gene Ontology (GO) and pathway enrichment analysis

GO and pathway enrichment analyses can demonstrate the importance of different biological processes and signaling pathways in the PPI network [22]. In this study, the DAVID platform version 6.8 (https://david-d.ncifcrf.gov) was used to perform GO enrichment and pathway enrichment analyses, and the results were displayed with network and bubble diagrams [22].

3 Results

3.1 The MXSGD and SARS-CoV-2 potential targets

A total of 272 MXSGD targets were obtained from TCMSP; Glycyrrhizae Radix Et Rhizoma (Gan Cao, 甘草) had 227 targets, Armeniacae Semen Amarum (Ku Xing Ren, 苦杏仁) had 71 targets, Ephedra Herba (Ma Huang, 麻黄) had 215 targets and Gypsum Fibrosum (Shi Gao, 石膏) had 0 targets. Meanwhile, a total of 21 targets related to SARS-CoV-2-infected cells were collected. There is some overlap between the MXSGD and the SARS-CoV-2 potential target sets (Figure 1).

The relationship between the compounds and potential targets of MXSGD is shown in Figure 2. This network is composed of 110 compound nodes, 251 target nodes, and 2 069 edges. In this network, some targets can be regulated by a lot of compounds: PTGS2 (94 edges), ESR1 (79 edges), CALM1 (75 edges), CALM2 (75 edges), CALM3 (75 edges), AR (70 edges) and NOS2 (69 edges). Some targets are also regulated by fewer compounds; PYGM, RAF1, RASA1, RASSF1 and RUNX1T1 are each regulated by one compound. Meanwhile, several compounds can regulate a lot of targets: Quercetin (145 edges), Kaempferol (62 edges), Luteolin (55 edges), 7-Methoxy-2-methyl isoflavone (43 edges), Formononetin (38 edges) and Isorhamnetin (35 edges). Several compounds can also regulate fewer targets: each of Icos-5-enoic acid, Gadelaidic acid and Mairin can only regulate one target.

3.2 Analysis of the MXSGD-SARS-CoV-2-PPI network

The MXSGD-SARS-CoV-2-PPI network consists of 272 nodes (241 MXSGD target nodes, 23 SARS-CoV-2 potential target nodes, and 8 MXSGD-2019nCoV target node) and 5 541 edges (Figure 3). The targets are arranged in descending order of Degree. The top 10 targets of each target group are: (1) MXSGD targets: AKT1 (163 edges), IL-6 (147 edges), MAPK3 (144 edges), TP53 (142 edges), TNF (134 edges), VEGFA (127 edges), JUN (122 edges), EGFR (121 edges), MAPK1 (118 edges) and MAPK8 (118 edges); (2) SARS-CoV-2 targets: CREB1 (99 edges), CCL5 (74 edges), CREBBP (62 edges), IRF3 (44 edges), IFNB1 (40 edges), LCN2 (29 edges), ATF2 (28 edges), IFNA1 (25 edges), MX1 (20 edges), BAG3 (18 edges) and

Table 1 Information of active compounds in MXSGD

Source	MOL ID	Compound name	Molecular weight	OB (%)	Caco-2	DL
Armeniacae Semen Amarum (Ku Xing Ren, 苦杏仁)	MOL010921	Estrone	270.4	53.56	1.01	0.32
	MOL002211	11,14-Eicosadienoic Acid	308.56	39.99	1.22	0.2
	MOL005030	Gondoic Acid	310.58	30.7	1.2	0.2
	MOL000953	Cholesterol	386.73	37.87	1.43	0.68
	MOL004355	Spinasterol	412.77	42.98	1.44	0.76
	MOL007207	Machiline	285.37	79.64	0.78	0.24
	MOL012922	L-Stepholidine	327.41	87.35	0.76	0.54
	MOL000449	Stigmasterol	412.77	43.83	1.44	0.76
	MOL000492	(+)-Catechin	290.29	54.83	– 0.03	0.24
	MOL000359	Sitosterol	414.79	36.91	1.32	0.75
	MOL000211	Mairin	456.78	55.38	0.73	0.78
	MOL002311	Glycyrol	366.39	90.78	0.71	0.67
	MOL004841	Licochalcone B	286.3	76.76	0.47	0.19
	MOL004908	Glabridin	324.4	53.25	0.97	0.47
	MOL005017	Phaseol	336.36	78.77	0.76	0.58
Ephedra Herba (Ma Huang, 麻黄)	MOL000422	Kaempferol	286.25	41.88	0.26	0.24
	MOL000098	Quercetin	302.25	46.43	0.05	0.28
	MOL004328	Naringenin	272.27	59.29	0.28	0.21
	MOL000449	Stigmasterol	412.77	43.83	1.44	0.76
	MOL000492	(+)-Catechin	290.29	54.83	– 0.03	0.24
	MOL010788	Leucopelargonidin	290.29	57.97	– 0.12	0.24
	MOL002823	Herbacetin	302.25	36.07	0.12	0.27
	MOL004798	Delphinidin	303.26	40.63	– 0.02	0.28
	MOL000006	Luteolin	286.25	36.16	0.19	0.25
	MOL000358	Beta-Sitosterol	414.79	36.91	1.32	0.75
	MOL001494	Mandenol	308.56	42	1.46	0.19
	MOL001755	24-Ethylcholest-4-En-3-One	412.77	36.08	1.46	0.76
	MOL001771	Poriferast-5-En-3beta-Ol	414.79	36.91	1.45	0.75
	MOL002881	Diosmetin	300.28	31.14	0.46	0.27
	MOL004576	Taxifolin	304.27	57.84	– 0.23	0.27
	MOL005043	Campesterol	400.76	37.58	1.32	0.71
	MOL005190	Eriodictyol	288.27	71.79	0.17	0.24
	MOL005573	Genkwanin	284.28	37.13	0.63	0.24
	MOL005842	Pectolinarigenin	314.31	41.17	0.7	0.3
	MOL011319	Truflex OBP	334.5	43.74	0.9	0.24
Glycyrrhizae Radix Et Rhizoma (Gan Cao, 甘草)	MOL001484	Inermine	284.28	75.18	0.89	0.54
	MOL001792	Liquiritigenin	256.27	32.76	0.51	0.18
	MOL000239	Jaranol	314.31	50.83	0.61	0.29
	MOL002565	Medicarpin	270.3	49.22	1	0.34

Table 1 Continued

Source	MOL ID	Compound name	Molecular weight	OB (%)	Caco-2	DL
	MOL000354	Isorhamnetin	316.28	49.6	0.31	0.31
	MOL003656	Lupiwighteone	338.38	51.64	0.68	0.37
	MOL003896	7-Methoxy-2-Methyl Isoflavone	266.31	42.56	1.16	0.2
	MOL000392	Formononetin	268.28	69.67	0.78	0.21
	MOL000417	Calycosin	284.28	47.75	0.52	0.24
	MOL004805	(2S)-2-[4-hydroxy-3-(3-methylbut-2-enyl)phenyl]-8,8-dimethyl-2,3-dihydropyrano[2,3-f]chromen-4-one (157414-03-4)	390.51	31.79	1	0.72
	MOL004806	Euchrenone	406.56	30.29	1.09	0.57
	MOL004808	Glyasperin B	370.43	65.22	0.47	0.44
	MOL004810	Glyasperin F	354.38	75.84	0.43	0.54
	MOL004811	Glyasperin C	356.45	45.56	0.71	0.4
	MOL004814	Isotrifoliol	298.26	31.94	0.53	0.42
	MOL004815	Kanzonol B	322.38	39.62	0.66	0.35
	MOL004820	Kanzonols W	336.36	50.48	0.63	0.52
Glycyrrhizae Radix Et Rhizoma (Gan Cao, 甘草)	MOL004824	(2S)-6-(2,4-Dihydroxyphenyl)-2-(2-Hydroxypropan-2-Yl)-4-Methoxy-2,3-Dihydrofuro[3,2-G]Chromen-7-One	384.41	60.25	0	0.63
	MOL004827	Semilicoisoflavone B	352.36	48.78	0.45	0.55
	MOL004828	Glepidotin A	338.38	44.72	0.79	0.35
	MOL004829	Glepidotin B	340.4	64.46	0.46	0.34
	MOL004833	Phaseolinisoflavan	324.4	32.01	1.01	0.45
	MOL004835	Glypallichalcone	284.33	61.6	0.76	0.19
	MOL004838	Kanzonol U	308.35	58.44	1	0.38
	MOL004848	Licochalcone G	354.43	49.25	0.64	0.32
	MOL004849	Licoarylcoumarin	368.41	59.62	0.4	0.43
	MOL004855	Licoricone	382.44	63.58	0.53	0.47
	MOL004856	Gancaonin A	352.41	51.08	0.8	0.4
	MOL004857	Gancaonin B	368.41	48.79	0.58	0.45
	MOL004863	Gancaonin L	354.38	66.37	0.52	0.41
	MOL004864	Gancaonin M	352.41	30.49	0.9	0.41
	MOL004866	Gancaonin O	354.38	44.15	0.48	0.41
	MOL004879	Glycyrin	382.44	52.61	0.59	0.47
	MOL004882	Licocoumarone	340.4	33.21	0.84	0.36
	MOL004883	Licoisoflavone A	354.38	41.61	0.37	0.42
	MOL004884	Licoisoflavone B	352.36	38.93	0.46	0.55
	MOL004885	Licoisoflavanone	354.38	52.47	0.39	0.54

Table 1 Continued

Source	MOL ID	Compound name	Molecular weight	OB (%)	Caco-2	DL
	MOL004891	Shinpterocarpin	322.38	80.3	1.1	0.73
	MOL004898	5-Prenylbutein	340.4	46.27	0.41	0.31
	MOL004904	Licopyranocoumarin	384.41	80.36	0.13	0.65
	MOL004907	Glyzaglabrin	298.26	61.07	0.34	0.35
	MOL004910	Glabranin	324.4	52.9	0.97	0.31
	MOL004911	Glabrene	322.38	46.27	0.99	0.44
	MOL004912	Glabrone	336.36	52.51	0.59	0.5
	MOL004913	Hedysarimcoumestan B	298.26	48.14	0.48	0.43
	MOL004914	1,3-Dihydroxy-8,9-Dimethoxy-6-Benzofurano[3,2-C]Chromenone	328.29	62.9	0.4	0.53
	MOL004915	Eurycarpin A	338.38	43.28	0.43	0.37
	MOL004935	Sigmoidin B	356.4	34.88	0.42	0.41
	MOL004941	(2R)-7-hydroxy-2-(4-hydroxyphenyl)chroman-4-one (578-86-9)	256.27	71.12	0.41	0.18
	MOL004945	Isobavachin	324.4	36.57	0.72	0.32
	MOL004948	Isoglycyrol	366.39	44.7	0.91	0.84
	MOL004949	Isolicoflavonol	354.38	45.17	0.54	0.42
Glycyrrhizae Radix Et Rhizoma (Gan Cao, 甘草)	MOL004957	Isoformononetin	268.28	38.37	0.79	0.21
	MOL004959	1-Methoxyphaseollidin	354.43	69.98	1.01	0.64
	MOL004961	Quercetin Der.	330.31	46.45	0.39	0.33
	MOL004966	3'-Hydroxy-4'-O-Methylglabridin	354.43	43.71	1	0.57
	MOL000497	Licochalcone A	338.43	40.79	0.82	0.29
	MOL004974	3'-Methoxyglabridin	354.43	46.16	0.94	0.57
	MOL004978	4'-Methoxyglabridin	338.43	36.21	1.12	0.52
	MOL004980	Inflacoumarin A	322.38	39.71	0.73	0.33
	MOL004985	Icos-5-Enoic Acid	310.58	30.7	1.22	0.2
	MOL004988	Kanzonol F	420.54	32.47	1.18	0.89
	MOL004989	6-Prenylated Eriodictyol	356.4	39.22	0.4	0.41
	MOL004990	7,2',4'-Trihydroxy-5-methoxy-3-arylcoumarin (ZINC105741014)	300.28	83.71	0.24	0.27
	MOL004991	7-Acetoxy-2-Methylisoflavone	294.32	38.92	0.74	0.26
	MOL004993	8-Prenylated Eriodictyol	356.4	53.79	0.43	0.4
	MOL004996	Gadelaidic Acid	310.58	30.7	1.2	0.2
	MOL000500	Vestitol	272.32	74.66	0.86	0.21
	MOL005000	Gancaonin G	352.41	60.44	0.78	0.39
	MOL005001	Gancaonin H	420.49	50.1	0.6	0.78
	MOL005003	Licoagrocarpin	338.43	58.81	1.23	0.58

Table 1 Continued

Source	MOL ID	Compound name	Molecular weight	OB (%)	Caco-2	DL
Glycyrrhizae Radix Et Rhizoma (Gan Cao, 甘草)	MOL005007	Glyasperins M	368.41	72.67	0.49	0.59
	MOL005008	Glycyrrhiza Flavonol A	370.38	41.28	– 0.09	0.6
	MOL005012	Licoagroisoflavone	336.36	57.28	0.71	0.49
	MOL005016	Odoratin	314.31	49.95	0.42	0.3
	MOL005018	Xambioona	388.49	54.85	1.09	0.87
	MOL005020	Dehydroglyasperins C	340.4	53.82	0.68	0.37
	MOL000359	Sitosterol	414.79	36.91	1.32	0.75
	MOL000211	Mairin	456.78	55.38	0.73	0.78
	MOL002311	Glycyrol	366.39	90.78	0.71	0.67
	MOL004841	Licochalcone B	286.3	76.76	0.47	0.19
	MOL004908	Glabridin	324.4	53.25	0.97	0.47
	MOL005017	Phaseol	336.36	78.77	0.76	0.58
	MOL000422	Kaempferol	286.25	41.88	0.26	0.24
	MOL000098	Quercetin	302.25	46.43	0.05	0.28
	MOL004328	Naringenin	272.27	59.29	0.28	0.21

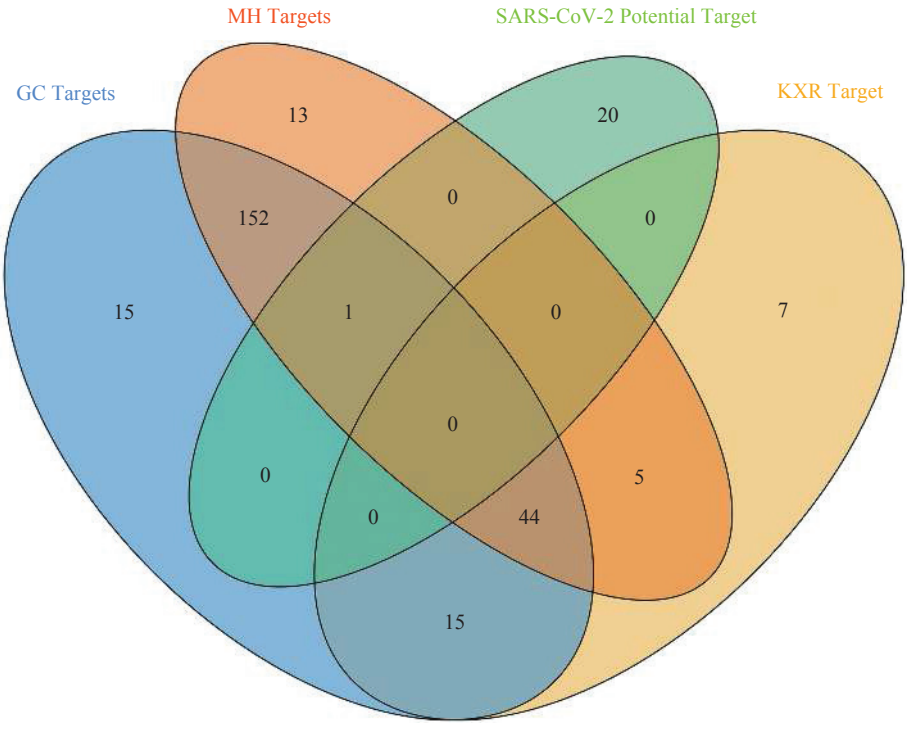

Figure 1 Venn diagram of MXSGD and SARS-CoV-2

GC represents Glycyrrhizae Radix Et Rhizoma (Gan Cao, 甘草); KXR represents Armeniacae Semen Amarum (Ku Xing Ren, 苦杏仁); MH represents Ephedra Herba (Ma Huang, 麻黄).

CASP6 (18 edges); (3) MXSGD-SARS-CoV-2 targets: CASP3 (123 edges), FOS (109 edges), IL10 (92 edges), CCL2 (92 edges), BCL2L1 (78 edges), IFNG (68 edges), CXCL10 (63 edges) and DPP4 (29 edges).

3.3 Biological processes of the MXSGD-SARS-CoV-2-PPI network

The MXSGD-SARS-CoV-2-PPI network was analyzed using MCODE, and 12 clusters were found (Table 2

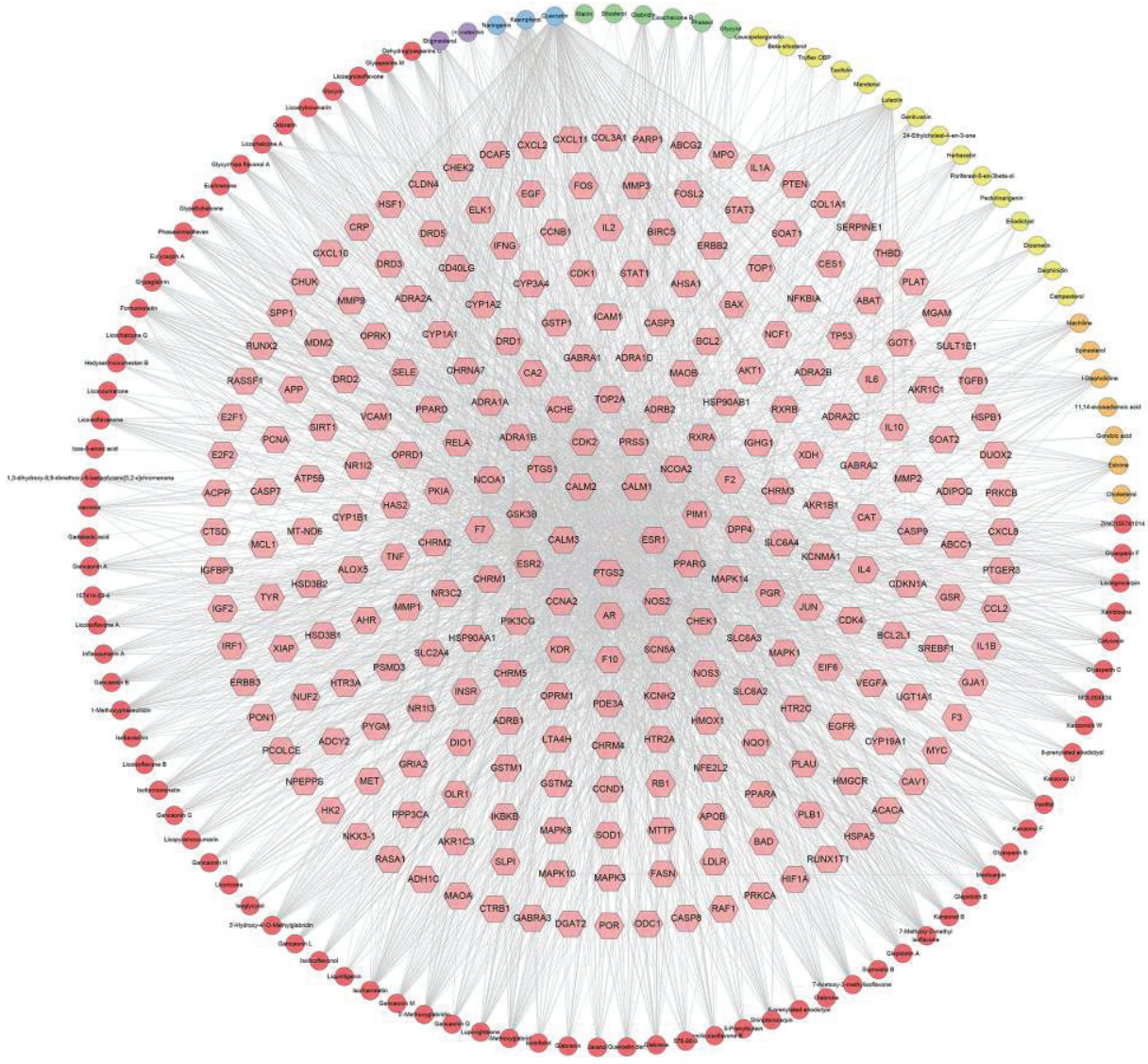

Figure 2 Compound-target network of MXSGD

Pink hexagons represent MXSGD targets. Red, orange and yellow circles represent compounds of Glycyrrhizae Radix Et Rhizoma (Gan Cao, 甘草), Armeniacae Semen Amarum (Ku Xing Ren, 苦杏仁) and Ephedra Herba (Ma Huang, 麻黄), respectively. Green circles represent common compounds of Glycyrrhizae Radix Et Rhizoma (Gan Cao, 甘草) and Armeniacae Semen Amarum (Ku Xing Ren, 苦杏仁). Blue circles represent common compounds of Glycyrrhizae Radix Et Rhizoma (Gan Cao, 甘草) and Ephedra Herba (Ma Huang, 麻黄). Purple circles represent common compounds of Armeniacae Semen Amarum (Ku Xing Ren, 苦杏仁) and Ephedra Herba (Ma Huang, 麻黄).

and Figure 4). The targets in the clusters were input into DAVID to perform GO enrichment analysis, and several biological processes were discovered.

Cluster 1 is related to inflammatory responses (inflammatory cells, inflammatory cytokines, and their signaling pathways), immune responses (T cells, monocytes, B cells and other immune cells), immune factors (including IFN-γ and TNF-α), virus defense, humoral immunity, and mucosal innate immune response. Cluster 2 is associated with leukocyte migration. Cluster 5 is involved in steroid metabolism. Cluster 3, 4, 6, 7, 8, 9, 10, 11 did not return any antiviral biological processes. The biological processes are shown in Figure 5 and Table 3.

3.4 Herb-Pathway-Target network analysis

The targets of the MXSGD-SARS-CoV-2-PPI network were input into DAVID to perform pathway enrichment analysis, and 10 antiviral signaling pathways were returned (Figure 6 and 7). Of the targets in this network, Glycyrrhizae Radix Et Rhizoma (Gan Cao, 甘草) could regulate 72, Ephedra Herba (Ma Huang, 麻黄) could regulate 70, and Armeniacae Semen Amarum (Ku Xing Ren, 苦杏仁) could regulate 13. This indicates that Ephedra Herba (Ma Huang, 麻黄) and Glycyrrhizae Radix Et Rhizoma (Gan Cao, 甘草) may have the most important antiviral properties, while Armeniacae Semen Amarum (Ku Xing Ren, 苦杏仁) may be supportive. The fold enrichment and *P* value, among

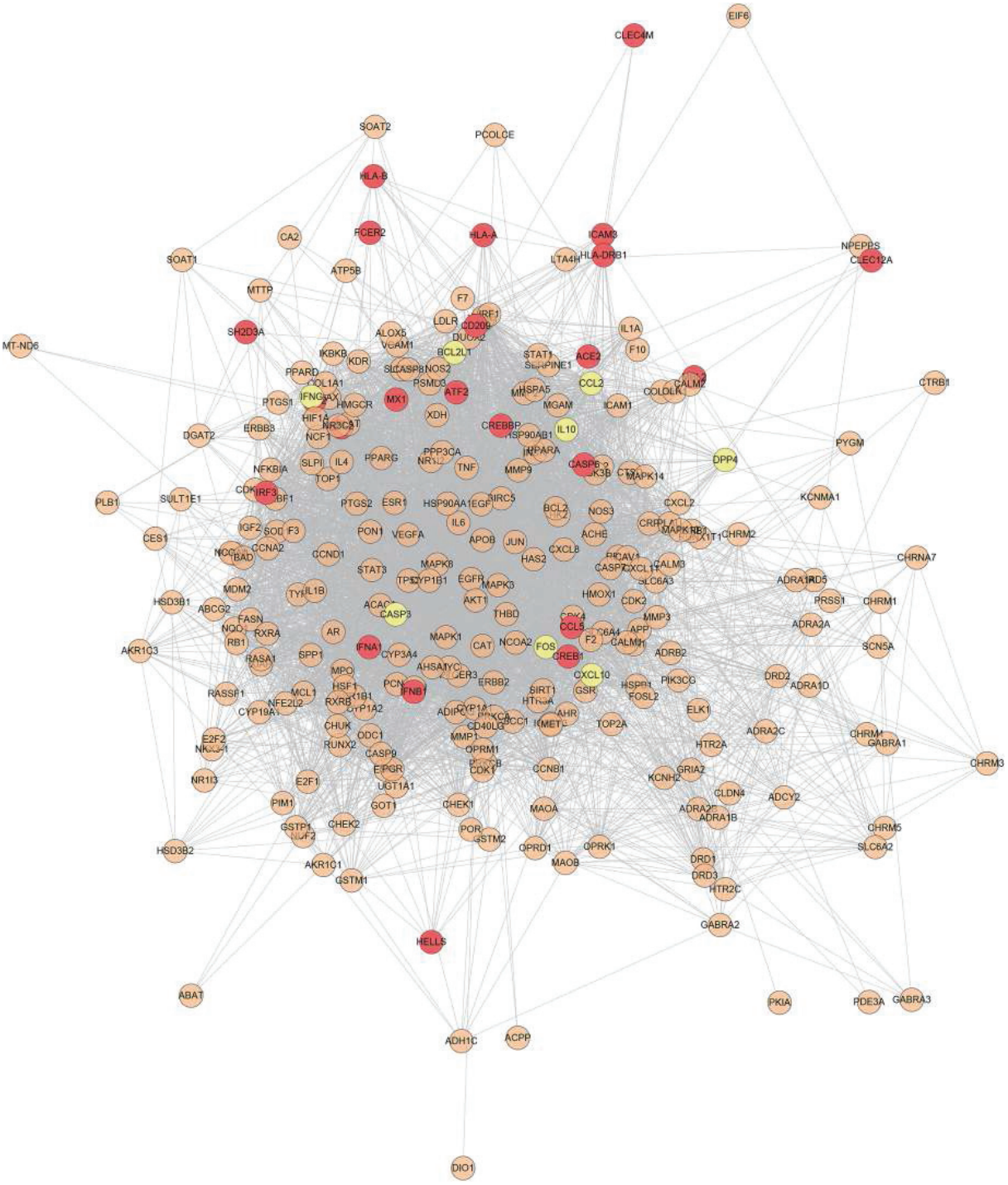

Figure 3 MXSGD-SARS-CoV-2-PPI network

Orange, red and yellow circles represent MXSGD, SARS-CoV-2 potential and MXSGD-SARS-CoV-2 targets, respectively.

others, of all signaling pathways are shown in Table 4 and Figure 7. The most important of those signaling pathways is the TNF, and Figure 8 shows that MXSGD can regulate multiple targets in the TNF pathway.

4 Discussion

This study used bioinformatics to construct and analyze the MXSGD compound-target, MXSGD-SARS-CoV-2-PPI and Herb-Pathway-Target networks. It revealed the multi-path and multi-molecular target mechanisms of MXSGD against COVID-19, which provides a basis for clinical use. In TCM, clinical diagnosis and treatment are based on syndrome differentiation. TCM associates the attributes of herbs with human meridians and collaterals and demonstrates the selectivity of herbs for the viscera to guide clinical practice [23]. Under the theoretical framework of TCM, COVID-19 belongs to the fiels of the plague of dampness pathogen. The

Table 2 Clusters of the MXSGD-SARS-CoV-2-PPI network

Cluster	Score	Nodes	Edges	Targets
1	48.49	62	1 479	MYC, IL1B, CXCL8, JUN, IL-4, TGFB1, SERPINE1, PTEN, MPO, RELA, PARP1, AKT1, TNF, CRP, MAPK8, SPP1, MMP1, STAT1, ICAM1, SELE, VCAM1, CXCL10, FOS, CASP3, CREB1, CCL2, IFNG, IL-10, BCL2L1, STAT3, CCND1, MAPK1, CCL5, EGFR, VEGFA, CDKN1A, CASP9, MMP2, MMP9, PTGS2, IL-6, HSP90AA1, TP53, CAT, MDM2, AR, PPARG, ERBB2, MAPK14, MCL1, IL-2, NOS2, CCNB1, CD40LG, NOS3, MAPK3, ADIPOQ, MMP3, PLAU, EGF, HMOX1, HIF1A
2	10.70	38	198	RB1, CDK4, CAV1, IFNB1, F3, GJA1, ESR1, SIRT1, HSPB1, NFKBIA, APP, CASP7, GSK3B, CDK2, BIRC5, IL1A, CHEK1, XIAP, CXCL2, CHEK2, KDR, MET, MAPK10, ESR2, RUNX2, SOD1, CDK1, CCNA2, PGR, IGF2, IRF1, IRF3, AHR, CREBBP, CASP8, RAF1, NFE2L2, HSPA5
3	10.38	17	83	OPRD1, LDLR, CHRM2, OPRK1, PTGER3, DRD2, PLAT, THBD, F2, CXCL11, ADRA2C, OPRM1, ADRA2B, ADCY2, DRD3, ADRA2A, CHRM4
4	7.50	9	30	MAOA, HTR2A, HTR3A, ADRA1A, HTR2C, ADRB1, ADRA1B, ADRA1D, SLC6A3
5	6.75	9	27	NR1I3, GSTM1, CYP1A1, AKR1C3, UGT1A1, CYP1B1, HSD3B2, HSD3B1, AKR1C1
6	3.33	4	5	PRKCB, ATF2, PRKCA, TOP2A
7	3.00	3	3	CTSD, NCOA1, NCOA2
8	3.00	3	3	DGAT2, ACACA, FASN
9	3.00	3	3	CYP1A2, NR1I2, CES1
10	3.00	3	3	SCN5A, KCNMA1, KCNH2
11	3.00	3	3	GRIA2, GABRA1, GABRA3
12	2.80	6	7	DRD5, MAOB, CHRM5, CHRM3, DRD1, CHRM1

etiology attribute is “pathogen of damp toxin”. The disease is localized in the lung and spleen, and the basic pathogenesis is characterized as “wet, poison, stasis and closure” [24]. The results of pathological anatomy also confirmed that the damage caused by the new coronavirus is mainly in the lungs [25].

By analyzing the MXSGD-SARS-CoV-2-PPI network, we found that some targets of MXSGD can interact with ACE (including ESR1, PTGS2, CAT, PPARG, NOS2, F2, NOS3, KDR, ADRA1B, ADRB2, ADRA1D, NR3C2, ACHE, SLC6A4, ADRB1, HMOX1, ADRA1A, PON1 and NPEPPS). Other targets can interact with ACE2 (CAT, NOS3, NR3C2, ACHE, LTA4H, NCF1, CDK4, IL-6, MAPK3, HIF1A, CRP, NPEPPS, CALM1, CALM2 and CALM3). Those indicate that MXSGD may regulate the expression of ACE2 receptors in various organs affected by COVID-19.

SARS-CoV-2 can induce inflammatory storms. When it infects the human body, it can invade cells through ACE2 [26]. The lung tissues that highly express ACE2 and are externally exposed become the main targets. Immune cells in the lung are over-activated, and they produce several inflammatory factors, such as interferon (IFN), interleukin (IL), chemokines, colony-stimulating factors (CSFs), tumor necrosis factor (TNF) [27]. These cytokines are secreted by certain immune cells, and they may promote or inhibit inflammation. They maintain a balanced state within the normal human body [28]. Pro-inflammatory factors can activate and recruit other immune cells. Immune cells can secrete more cytokines and activate and recruit more immune cells, thus forming a positive feedback loop that leads to an inflammation storm. Eventually, several immune cells and the interstitial fluid accumulate in the lungs, which block the gas exchange between alveoli and capillaries, resulting in acute respiratory distress syndrome and death in many patients [29]. The current study found that MXSGD can regulate inflammatory responses (GO:0006954, GO:0050727, GO:0002674), immune factors and their mediated pathways (including IFN-γ, TNF-α, IL-1 and IL-6) (GO:0071347), and the activation, proliferation and chemotaxis of immune cells (macrophages, T cells, B cells, white blood cells and so on) (such as GO:0050852, GO:0042110, GO:0010818, GO:0030225, GO:0006955). Our previous research also showed that MXSGD can effectively reduce lung inflammation, protect immune organs and regulate cytokine balance, which constitute the possible mechanisms for alleviating lung injury in mice caused by the inhibition of the TLR4-MyD88-TRAF6 signaling pathway by influenza

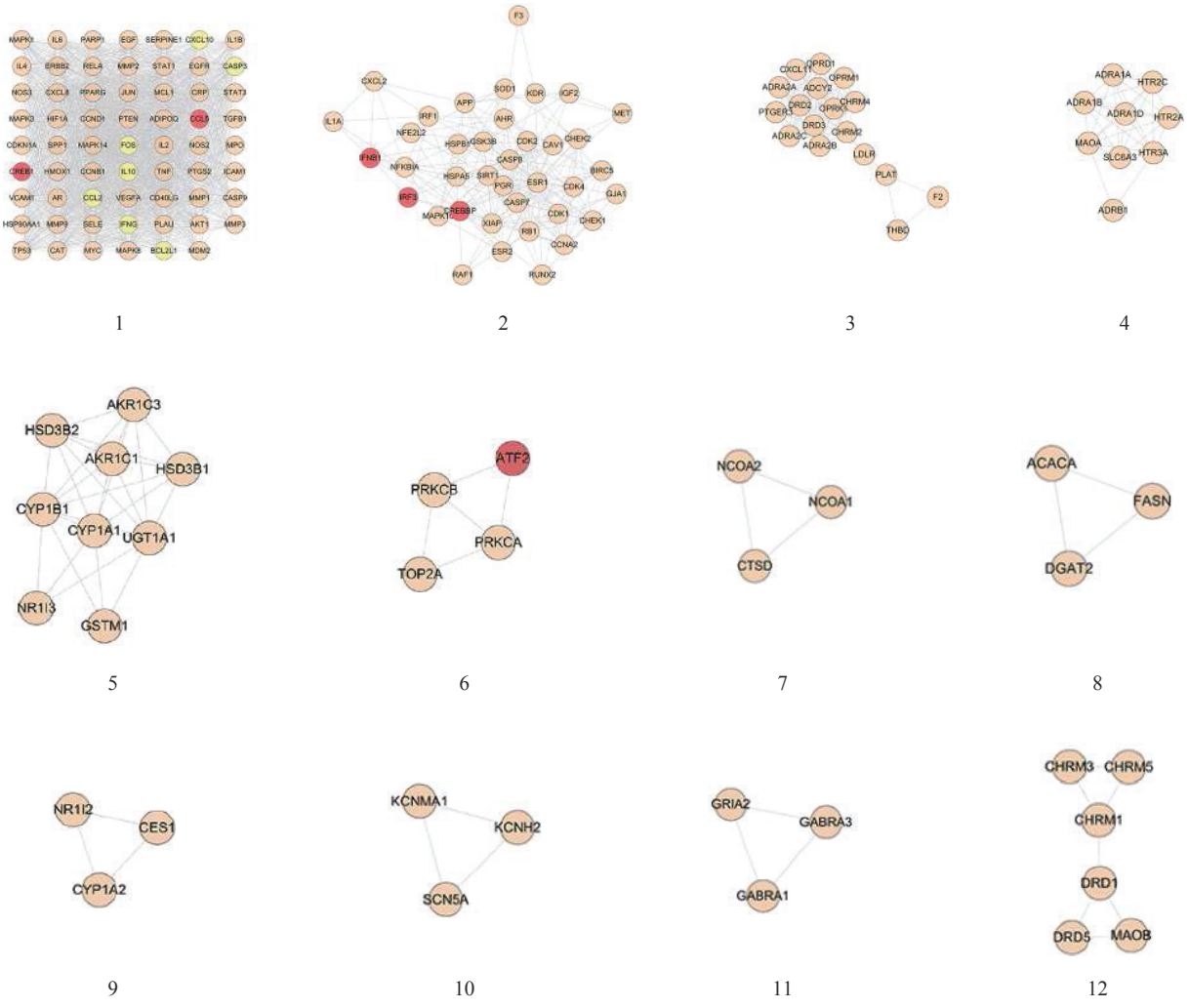

Figure 4 Clusters of the MXSGD-SARS-CoV-2-PPI network

Orange, red and yellow circles represent MXSGD, SARS-CoV-2 and MXSGD-SARS-CoV-2 targets, respectively.

A viruses [9]. Recent studies have shown that patients with COVID-19 often have concomitant influenza and parainfluenza virus infections, especially in severe cases; hence, treatment for multiple infections is required. Our previous research provided valuable insights into the antiviral and antibacterial properties of MXSGD; it revealed that MXSGD can inhibit the replication of the influenza virus by regulating the body's immunity [30]. In addition, the results of pathway enrichment analysis showed that MXSGD can inhibit immune factors and prevent excessive immune response by regulating the TNF, NOD-like receptor, FoxO, PI3K-AKT, Toll-like receptor, T cell receptor, NF-kappa B, B cell receptor and Jak-STAT signaling pathways, as well as Fc gamma R-mediated phagocytosis.

According to the current "Diagnosis and Treatment Protocol for COVID-19" (Trial Version 5 - 7) issued by the National Health Commission, MXSGD is recommended for the treatment of severe cases (especially for the patients with the syndrome of epidemic virus attacking lung) [31]. Recent studies have shown that severe cases have a higher proportion of cytokine storms, leading to worse prognoses [32]. Examination of blood cytokines in severe cases revealed that the D-dimer increase, while peripheral blood lymphocytes progressively decrease; their cytokines IL-2, IL-7, IL-10, GCSF, IP10, MCP1, MIP1A and TNF-α are also higher than normal [33]. Such high levels of pro-inflammatory cytokines may cause shock and damage to the heart, liver and kidneys, as well as respiratory or multiple organ failure. The aforementioned cytokines also extensively mediate lung pathological changes, which may result in extensive infiltration of neutrophils and macrophages, and subsequent diffuse alveolar injury [34, 35].

WEI et al. [36] conducted a comprehensive immunological analysis of the blood samples of 33 COVID-19 patients and found the key mechanism for the inflammatory storm. After SARS-CoV-2 infection, pathogenic T cells are rapidly activated, producing cytokines such as GM-CSF and IL-6. GM-CSF further activates CD14+ and CD16+ inflammatory monocytes, thereby producing a large amount of IL-6 and

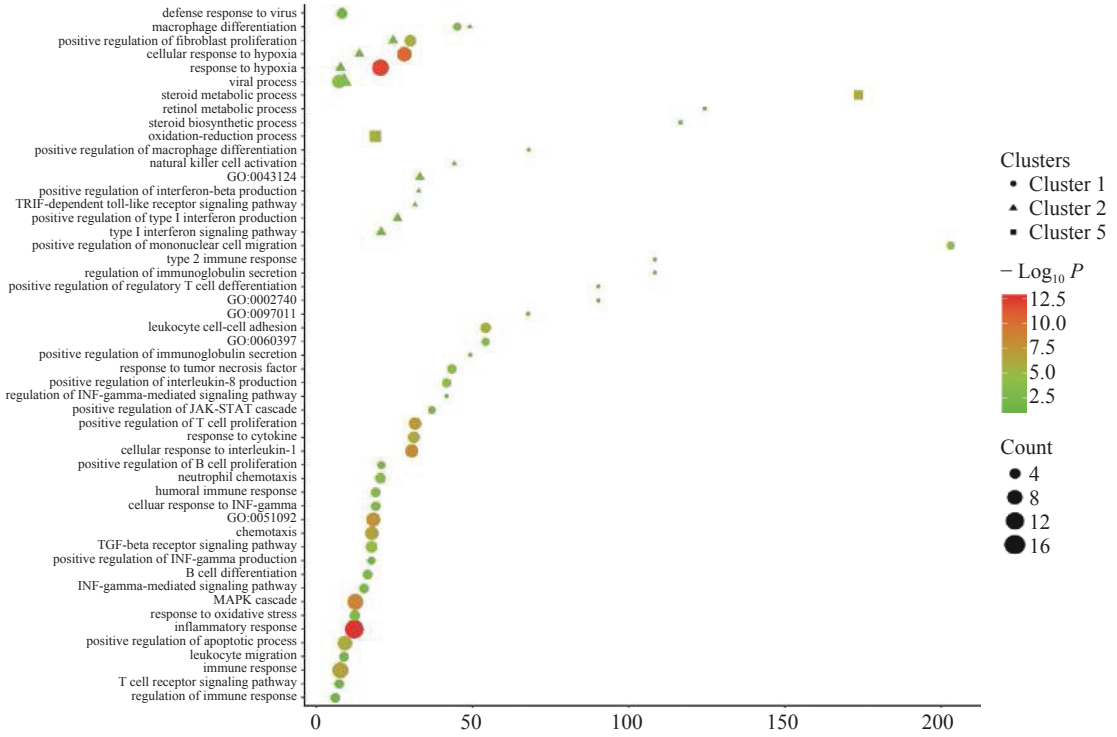

Figure 5 Bubble chart of biological processes

x axis represents fold enrichment.

Table 3 Biological processes of the MXSGD-SARS-CoV-2-PPI network

Clusters	Term	Biological processes	*P* value	Targets	Fold enrichment
Cluster 1	GO:0006954	Inflammatory response	2.66×10^{-13}	IL-6, TNF, CCL2, PTGS2, RELA, CRP, CXCL8, CCL5, IL-10, TGFB1, CXCL10, AKT1, FOS, CD40LG, IL1B, SELE, SPP1	12.15
	GO:0001666	Response to hypoxia	1.02×10^{-12}	CCL2, CREB1, MMP2, ADIPOQ, TGFB1, VCAM1, CASP3, HIF1A, HMOX1, VEGFA, NOS2, CAT, PLAU	20.47
	GO:0071456	Cellular response to hypoxia	6.04×10^{-11}	CCNB1, AKT1, ICAM1, HIF1A, PTGS2, HMOX1, VEGFA, TP53, MDM2, PTEN	28.21
	GO:0000165	MAPK cascade	2.27×10^{-9}	EGFR, MAPK1, TNF, CCL2, ERBB2, MAPK3, IL1B, CCL5, EGF, MYC, TGFB1, IL-22	12.40
	GO:0071347	Cellular response to interleukin-1	6.49×10^{-9}	ICAM1, IL-6, HIF1A, CCL2, RELA, CXCL8, CCL5, MYCYC	30.52
	GO:0051092	Positive regulation of NF-kappaB Transcription factor activity	2.59×10^{-8}	ICAM1, AR, IL-6, TNF, CD40LG, RELA, IL1B, CAT, TGFB1	18.33
	GO:0042102	Positive regulation of T cell proliferation	7.68×10^{-8}	IL-4, VCAM1, IL-6, CD40LG, IFNG, IL1B, CCL5	31.60
	GO:0006935	Chemotaxis	2.83×10^{-7}	IL-4, MAPK1, CCL2, MAPK14, CXCL8, CCL5, PLAU, CXCL1010	17.76
	GO:0006955	Immune response	2.92×10^{-7}	IL-4, IL6, TNF, CCL2, CD40LG, IFNG, CXCL8, IL1B, CCL5, IL-10, CXCL10, IL-2	7.72
	GO:0034097	Response to cytokine	1.22×10^{-6}	IL-4, FOS, MCL1, JUN, BCL2L1, STAT1	31.25

Table 3 Continued

Clusters	Term	Biological processes	*P* value	Targets	Fold enrichment
Cluster 1	GO:0043065	Positive regulation of apoptotic process	1.26×10^{-6}	AKT1, IL-6, TNF, PTGS2, HMOX1, CREB1, TP53, MAPK8, BCL2L1, TGFB1	9.03
	GO:0048146	Positive regulation of fibroblast proliferation	1.48×10^{-6}	CCNB1, EGFR, CDKN1A, JUN, MYC, TGFB1	30.09
	GO:0007159	Leukocyte cell-cell adhesion	1.88×10^{-6}	VCAM1, ICAM1, CD40LG, CCL5, SELE	54.17
	GO:0007179	Transforming growth factor beta receptor signaling pathway	2.07×10^{-5}	FOS, CCL2, JUN, CREB1, PARP1, TGFB1	17.66
	GO:0071677	Positive regulation of mononuclear cell migration	7.75×10^{-5}	IIL-4, TNF, TGFB11	203.13
	GO:0030593	Neutrophil chemotaxis	9.6×10^{-5}	CCL2, IFNG, CXCL8, IL1B, CCL5	20.52
	GO:0034612	Response to tumor necrosis factor	9.91×10^{-5}	CASP3, PTGS2, ADIPOQ, SELE	43.33
	GO:0016032	Viral process	1.01×10^{-4}	VCAM1, MAPK1, CREB1, MAPK3, TP53, MDM2, MMP1, STAT3	7.25
	GO:0032757	Positive regulation of interleukin-8 production	1.12×10^{-4}	TNF, SERPINE1, IL1B, ADIPOQ	41.67
	GO:0006979	Response to oxidative stress	6.83×10^{-4}	AKT1, EGFR, PTGS2, HMOX1, MPO	12.31
	GO:0006959	Humoral immune response	1.16×10^{-3}	IL-6, TNF, CCL2, IFNG	19.01
	GO:0071346	Cellular response to interferon-gamma	1.16×10^{-3}	CCL2, NOS2, CCL5, MYC	19.01
	GO:0060397	JAK-STAT cascade involved in growth hormone signaling pathway	1.32×10^{-3}	MAPK1, MAPK3, STAT3	54.17
	GO:0030183	B cell differentiation	1.77×10^{-3}	IL-4, VCAM1, CD40LG, IL-100	16.41
	GO:0030225	Macrophage differentiation	1.91×10^{-3}	MMP9, VEGFA, PARP1	45.14
	GO:0060333	Interferon-gamma-mediated signaling pathway	2.19×10^{-3}	VCAM1, ICAM1, IFNG, STAT1	15.26
	GO:0046427	Positive regulation of JAK-STAT cascade	2.86×10^{-3}	IIL-6, CCL5, IL-100	36.93
	GO:0051607	Defense response to virus	3.04×10^{-3}	IL-IL-6, RELA, IFNG, STAT1, CXCL100	8.21
	GO:0030890	Positive regulation of B cell proliferation	8.82×10^{-3}	IL-4, CDKN1A, IL-2	20.83
	GO:0050900	Leukocyte migration	9.91×10^{-3}	ICAM1, MMP9, SELE, MMP1	8.88
	GO:0032729	Positive regulation of interferon-gamma production	1.21×10^{-2}	TNF, IL1B, IL-2	17.66
	GO:0050852	T cell receptor signaling pathway	1.66×10^{-2}	MAPK1, RELA, IFNG, PTEN	7.32
	GO:0051023	Regulation of immunoglobulin secretion	1.80×10^{-2}	TNF, CD40LG	108.34

Table 3 Continued

Clusters	Term	Biological processes	*P* value	Targets	Fold enrichment
Cluster 1	GO:0042092	Type 2 immune response	1.80×10^{-2}	IL-4, IL-100	108.34
	GO:0002740	Negative regulation of cytokine secretion involved in the immune response	2.16×10^{-2}	TNF, IL-10	90.28
	GO:0045591	Positive regulation of regulatory T cell differentiation	2.16×10^{-2}	TGFB1, IL-2	90.28
	GO:0050776	Regulation of immune response	2.69×10^{-2}	IL-4, VCAM1, ICAM1, CD40LGG	6.09
	GO:0097011	Cellular response to granulocyte-macrophage colony-stimulating factor stimulus	2.87×10^{-2}	AKT1, MAPK1	67.71
	GO:0051024	Positive regulation of immunoglobulin secretion	3.93×10^{-2}	IL-6, IL-2	49.24
	GO:0060334	Regulation of interferon-gamma-mediated signaling pathway	4.62×10^{-2}	IFNG, STAT1	41.67
Cluster 2	GO:0016032	Viral process	4.73×10^{-4}	CREBBP, NFKBIA, RB1, CCNA2, SIRT1, KDR	8.87
	GO:0043124	Negative regulation of I-kappaB kinase/NF-kappaB signaling	3.50×10^{-3}	CASP8, ESR1, SIRT1	33.14
	GO:0032481	Positive regulation of type I interferon production	5.63×10^{-3}	CREBBP, IRF1, IRF3	25.99
	GO:0048146	Positive regulation of fibroblast proliferation	6.29×10^{-3}	ESR1, CDK4, CCNA2	24.55
	GO:0060337	Type I interferon signaling pathway	8.74×10^{-3}	IFNB1, IRF1, IRF3	20.71
	GO:0071456	Cellular response to hypoxia	1.89×10^{-2}	NFE2L2, CCNA2, SIRT1	13.81
	GO:0045651	Positive regulation of macrophage differentiation	2.83×10^{-2}	CASP8, RB1	67.98
	GO:0030225	Macrophage differentiation	3.89×10^{-2}	CASP8, SIRT1	49.10
	GO:0030101	Natural killer cell activation	4.32×10^{-2}	IFNB1, CASP8	44.19
	GO:0051607	Defense response to virus	5.11×10^{-2}	IFNB1, IRF1, IRF3	8.03
	GO:0001666	Response to hypoxia	5.50×10^{-2}	CAV1, CREBBP, RAF1	7.71
	GO:0032728	Positive regulation of interferon-beta production	5.79×10^{-2}	IRF1, IRF3	32.73
	GO:0035666	TRIF-dependent toll-like receptor signaling pathway	5.99×10^{-2}	CASP8, IRF3	31.56
Cluster 5	GO:0008202	Steroid metabolic process	8.68×10^{-7}	AKR1C3, CYP1B1, CYP1A1, UGT1A1	173.56
	GO:0055114	Oxidation-reduction process	2.75×10^{-6}	AKR1C3, HSD3B2, HSD3B1, CYP1B1, CYP1A1, AKR1C1	18.91
	GO:0042572	Retinol metabolic process	1.42×10^{-2}	AKR1C3, CYP1B1	124.39
	GO:0006694	Steroid biosynthetic process	1.51×10^{-2}	HSD3B2, HSD3B1	116.61

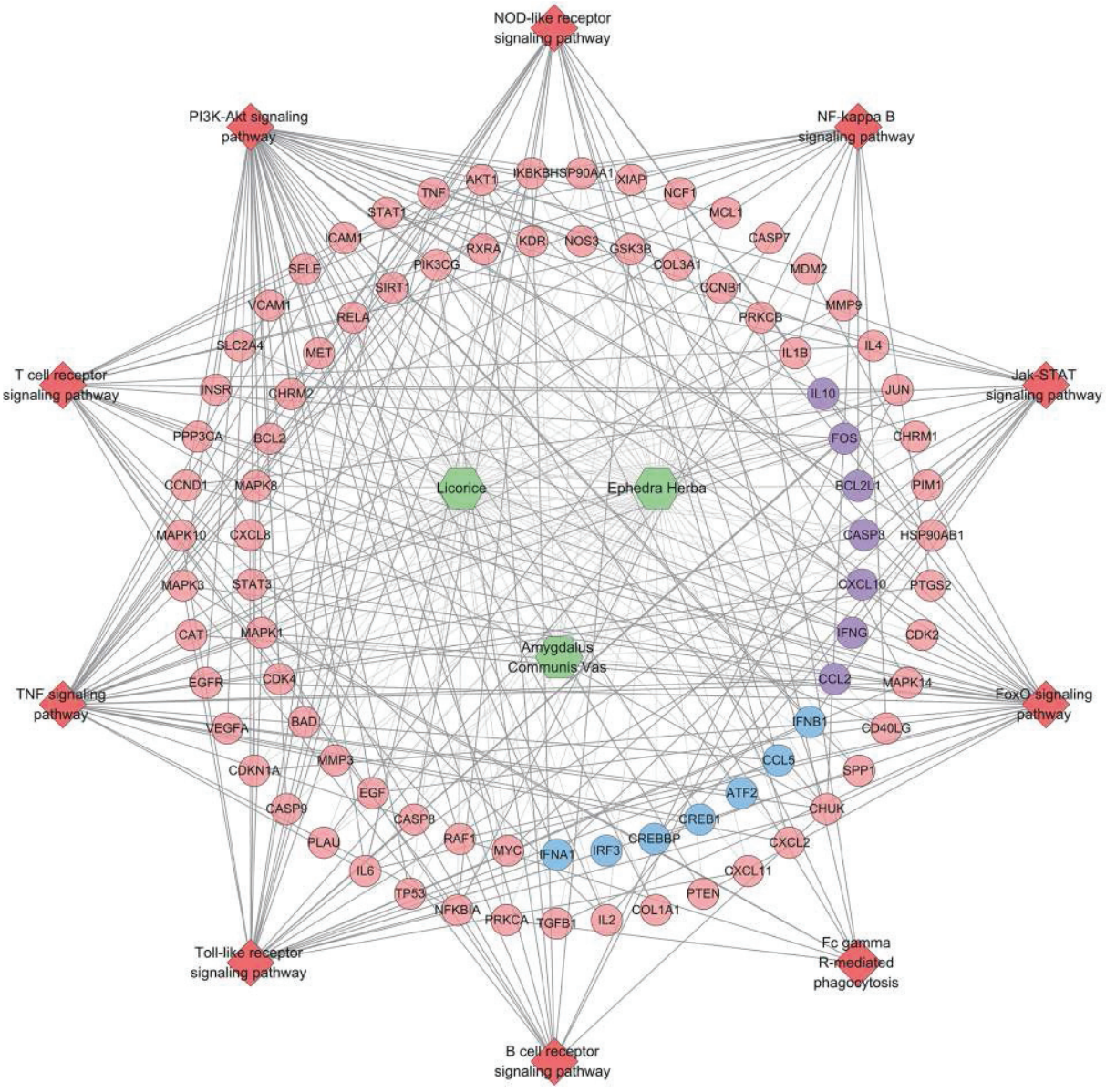

Figure 6 Herb-Pathway-Target network

Pink, blue and purple circles represent MXSGD, SARS-CoV-2 and MXSGD-SARS-CoV-2 targets, respectively. Red diamonds represent signaling pathways. Green hexagons represent herbs.

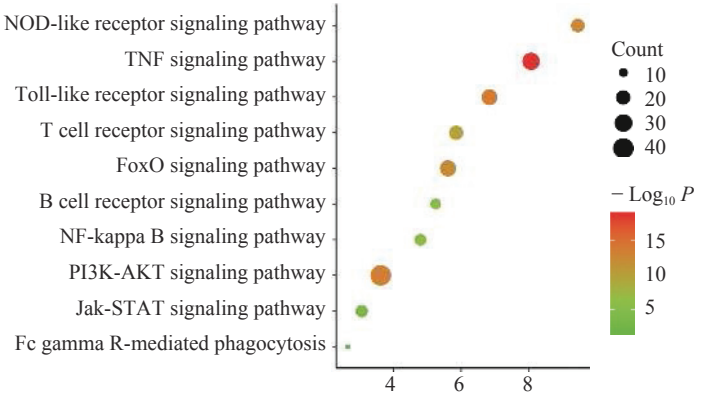

Figure 7 Bubble chart of signaling pathways

x axis represents fold enrichment.

Table 4 Signaling pathways of the MXSGD-SARS-CoV-2-PPI network

Term	Signaling pathways	*P* value	Genes	Fold enrichment
hsa04668	TNF signaling pathway	1.80×10^{-19}	CCL2, TNF, PTGS2, MMP9, CXCL2, NFKBIA, MMP3, CCL5, CXCL10, ATF2, VCAM1, AKT1, FOS, CASP3, CASP7, CASP8, IL1B, CHUK, PIK3CG, ICAM1, IL-6, RELA, CREB1, MAPK10, MAPK1, JUN, MAPK14, MAPK3, MAPK8, IKBKB, SELE	8.07
hsa04620	Toll-like receptor signaling pathway	2.00×10^{-14}	TNF, CXCL8, NFKBIA, CXCL11, CCL5, CXCL10, AKT1, FOS, IFNA1, CASP8, IL1B, CHUK, SPP1, PIK3CG, IL-6, RELA, MAPK10, STAT1, MAPK1, IFNB1, MAPK14, JUN, MAPK3, MAPK8, IRF3, IKBKB	6.83
hsa04151	PI3K-AKT signaling pathway	5.23×10^{-14}	HSP90AB1, MCL1, COL3A1, BCL2L1, PTEN, ATF2, AKT1, IFNA1, CASP9, BCL2, NOS3, EGF, INSR, MYC, CHUK, SPP1, PRKCA, IL-4, PIK3CG, EGFR, IL-6, HSP90AA1, CREB1, RELA, RXRA, MET, TP53, RAF1, BAD, CDK4, CDK2, KDR, MAPK1, CCND1, CDKN1A, IFNB1, CHRM2, GSK3B, CHRM1, MAPK3, VEGFA, MDM2, COL1A1, IKBKB, IL-2	3.63
hsa04621	NOD-like receptor signaling pathway	3.11×10^{-13}	HSP90AB1, IL-6, TNF, CCL2, HSP90AA1, RELA, CXCL2, CXCL8, NFKBIA, MAPK10, CCL5, MAPK1, MAPK14, CASP8, MAPK3, IL1B, MAPK8, IKBKB, CHUK	9.45
hsa04068	FoxO signaling pathway	8.05×10^{-13}	PTEN, IL-10, TGFB1, AKT1, SLC2A4, CAT, EGF, INSR, CHUK, EGFR, PIK3CG, IL-6, CREBBP, RAF1, MAPK10, SIRT1, CDK2, STAT3, CCNB1, MAPK1, CDKN1A, CCND1, MAPK14, MAPK3, MDM2, MAPK8, IKBKB	5.61
hsa04660	T cell receptor signaling pathway	2.26×10^{-10}	IL-4, PIK3CG, TNF, RELA, RAF1, NFKBIA, CDK4, IL-10, AKT1, FOS, MAPK1, CD40LG, JUN, GSK3B, MAPK14, IFNG, MAPK3, PPP3CA, IKBKB, CHUK, IL-2	5.85
hsa04064	NF-kappa B signaling pathway	2.03×10^{-6}	ICAM1, TNF, XIAP, PTGS2, RELA, NFKBIA, CXCL8, BCL2L1, VCAM1, CD40LG, BCL2, IL1B, IKBKB, CHUK, PLAU	4.80
hsa04662	B cell receptor signaling pathway	4.81×10^{-6}	PIK3CG, AKT1, FOS, MAPK1, JUN, GSK3B, RELA, MAPK3, RAF1, NFKBIA, PPP3CA, IKBKB, CHUK	5.25
hsa04630	Jak-STAT signaling pathway	1.95×10^{-4}	IL-4, PIK3CG, IL-6, CREBBP, PIM1, BCL2L1, STAT1, IL-10, STAT3, AKT1, IFNA1, CCND1, IFNB1, IFNG, MYC, IL-2	3.07
hsa04666	Fc gamma R-mediated phagocytosis	3.01×10^{-2}	PRKCA, PIK3CG, AKT1, MAPK1, NCF1, MAPK3, RAF1, PRKCB	2.65

other inflammatory factors. This facilitates the formation of an inflammatory storm and results in severe lung and immune system damage [37]. Therefore, IL-6 and GM-CSF are the two key inflammatory factors that trigger the inflammatory storm in patients with COVID-19 [38].

In summary, the main mechanism of MXSGD in the treatment of patients with severe COVID-19 pneumonia is the regulation of biological modules, such as the inflammatory and immune biological modules. Our previous studies demonstrated the inhibition of inflammatory storms in the H1N1 influenza mouse model by MXSGD. A recent research also showed that Lian Hua Qing Wen Capsule, composed of MXSGD and Yin Qiao Powder, can significantly inhibit the replication of SARS-CoV-2 in Vero E6 cells at the mRNA level and the production of pro-inflammatory cytokines (TNF-α, IL-6, CCL-2/MCP-1 and CXCL-10/IP-10) [39]. In addition, Lian Hua Qing Wen Capsule treatment can cause abnormal morphological changes within virus particles in the cells [39].

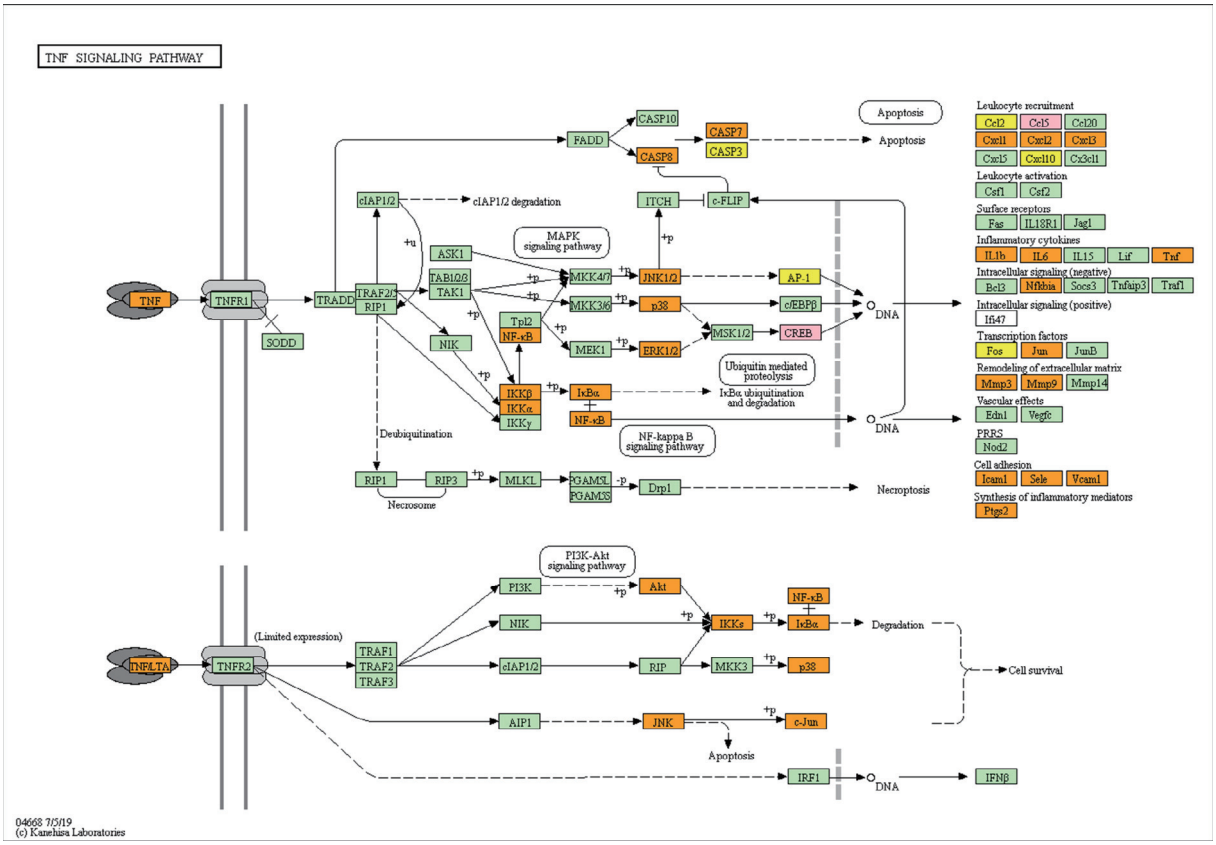

Figure 8 TNF pathway modified from hsa04668

Orange, pink and yellow represent MXSGD, SARS-CoV-2 and MXSGD-SARS-CoV-2 targets, respectively.

More importantly, our previous research on influenza A virus found that, the MXSGD clinical equivalent dose, and twice of it, can reduce the levels of TNF-α and IL-4, significantly increase the thymus and spleen indexes, and improve the pathological damage of the lung tissues [40]. In the comprehensive management of COVID-19, MXSGD and its modified formulae are mainly used in critically ill patients. A cascade of inflammatory events occur in patients, and leveraging multiple mechanisms to counteract their effects is crucial to patient recovery and survival. This systematic pharmacological study and previous studies have revealed the underlying mechanisms of MXSGD in the regulation of the biological module of inflammation. Therefore, this study provides important evidence for the clinical use of MXSGD in the treatment of severely ill patients with COVID-19.

5 Conclusions

MXSGD can control disease progression by regulating multiple compounds and targets; it can reduce inflammation and balance immunity by regulating several proteins interacting with ACE2 and a series of signaling pathways closely related to disease development. This study provides evidence to facilitate further research into MXSGD and its clinical adoption for the treatment of COVID-19.

Acknowledgements

We thank for the funding support from the National Natural Science Foundation of China (No. 81774126 and No. 81973670), the Natural Science Foundation of Hunan Province (No. 2016JJ2095 and No. 2017JJ3232), Scientific Research Project of Traditional Chinese Medicine for the Prevention and Treatment of New Pneumonia in Hunan Province (No. GYGG007), the Construction Project of Specialty of Traditional Chinese Medicine in Guangdong Province, and the Construction Project of Specialty of Traditional Chinese Medicine in Shenzhen.

Competing Interests

The authors declare no conflict of interest.

References

[1] HUI DS, MADANI T, NTOUMI F, et al. The continuing 2019-nCoV epidemic threat of novel coronaviruses to global health - the latest 2019 novel coronavirus outbreak in Wuhan, China. International Journal of Infectious Diseases, 2020, 91: 264–266.

[2] THE LANCET. Emerging understandings of 2019-nCoV. Lancet, 2020, 395(10221): 311.

[3] LUO Y, WANG CZ, HESSE-FONG J, et al. Application of Chinese medicine in acute and critical medical conditions. The American Journal of Chinese Medicine, 2019, 47(6): 1223–1235.

[4] FENG X, DUAN XJ, ZHANG B, et al. Analysis of programs and guidelines on traditional Chinese medicine (TCM) for COVID-19 to provide suggestions for future development of TCM clinical practice guidelines. Chinese Journal of Experimental Traditional Medical Formulae, 2020: 1-7 [2020-03-06]. https://doi.org/10.13422/j.cnki.syfjx.20200841.

[5] WANG D, YAN KK, CAO Q, et al. Study on the medication regularity of traditional Chinese medicine in the prevention of novel coronavirus pneumonia in various regions based on data mining. Journal of Chinese Medicinal Materials, 2020, 43(4): 1035–1040.

[6] LU FG, HE YC, XIAO ZZ, et al. Study on effect target of Maxing Shigan Decoction on anti-influenza virus A *in vitro*. Journal of Traditional Chinese Medicine University of Hunan, 2008, 28(2): 5–9.

[7] ZHANG W, LU FG, HE YC, et al. Experimental study on effect of Maxingshigan Dectoctin on anti-influenza virus a *in vitro*. Practical Preventive Medicine, 2007, 14(5): 1351–1353.

[8] ZHANG SY, HE GL, LU FG, et al. Mechanism research of anti influenza virus of ephedra decocted earlier Maxing Shigan Decoction from the expression level of IFN-α/β protein mediated by TLR7/8. China Journal of Traditional Chinese Medicine and Pharmacy, 2019, 34(3): 1188–1193.

[9] LI L, WEI K, LU FG, et al. Effect of Maxing Shigan Decoction against type A influenza virus infection in mice induced by viral lung injury based on TLR4-MyD88-TRAF6 signal pathways. Chinese Traditional and Herbal Drugs, 2017, 48(8): 1591–1596.

[10] ZENG LT, YANG KL. Exploring the pharmacological mechanism of Yanghe Decoction on HER2-positive breast cancer by a network pharmacology approach. Journal of Ethnopharmacology, 2017, 199: 68–85.

[11] ZENG LT, YANG KL, GE JW. Uncovering the pharmacological mechanism of astragalus salvia compound on pregnancy-induced hypertension syndrome by a network pharmacology approach. Scientific Reports, 2017, 7(1): 1–11.

[12] BAO TT, YANG KL, LONG ZY, et al. Systematic pharmacological methodology to explore the pharmacological mechanism of Siwu Decoction for osteoporosis. Medical Science Monitor: International Medical Journal of Experimental and Clinical Research, 2019, 25: 8152.

[13] CHEN CYC. TCM Database@Taiwan: the world's largest traditional Chinese medicine database for drug screening in silico. PLoS One, 2011, 6(1): e15939.

[14] RU JL, LI P, WANG JN, et al. TCMSP: a database of systems pharmacology for drug discovery from herbal medicines. Journal of Cheminformatics, 2014, 6(1): 13.

[15] XU X, ZHANG WX, HUANG C, et al. A novel chemometric method for the prediction of human oral bioavailability. International Journal of Molecular Sciences, 2012, 13(6): 6964–6982.

[16] ANO R, KIMURA Y, SHIMA M, et al. Relationships between structure and high-throughput screening permeability of peptide derivatives and related compounds with artificial membranes: application to prediction of Caco-2 cell permeability. Bioorganic & Medicinal Chemistry, 2004, 12(1): 257–264.

[17] HU GX, ZHANG CH, ZHAO WN, et al. QSPR study on the permeability of drugs across Caco-2 monolayer. Journal of Zhejiang University (Science Edition), 2009, 36(3): 304–308.

[18] HAMOSH A, SCOTT AF, AMBERGER JS, et al. Online Mendelian Inheritance in Man (OMIM), a knowledgebase of human genes and genetic disorders. Nucleic Acids Research, 2005, 33(SI): D51–D517.

[19] STELZER G, ROSEN N, PLASCHKES I, et al. The GeneCards Suite: from gene data mining to disease genome sequence analyses. Current Protocols in Human Genetics, 2016, 54(1): 1.30.1–1.30.33.

[20] SZKLARCZYK D, FRANCESCHINI A, WYDER S, et al. STRING v10: protein-protein interaction networks, integrated over the tree of life. Nucleic Acids Research, 2015, 43(D1): D447–D452.

[21] MISSIURO PV, LIU KS, ZOU LH, et al. Information flow analysis of interactome networks. PLoS Computational Biology, 2009, 5(4): e1000350.

[22] HUANG DW, SHERMAN BT, LEMPICKI RA, et al. Systematic and integrative analysis of large gene lists using DAVID bioinformatics resources. Nature Protocols, 2009, 4(1): 44–57.

[23] SU SB, JIA W, LU AP, et al. Evidence-based ZHENG: a traditional Chinese medicine syndrome 2013. Evidence-Based Complementary and Alternative Medicine, 2014, 2014: 484201.

[24] GU M, LIU J, SHI NN, et al. Analysis of property and efficacy of traditional Chinese medicine in staging prevention and treatment of corona virus disease 2019. China Journal of Chinese Materia Medica, 2020, 45(6): 1253–1258.

[25] LIU L. Novel coronavirus pneumonia death corpse system anatomy general observation report. Chinese Journal of Forensic Medicine, 2020, 36(1): 19–21.

[26] KUBA K, IMAI Y, RAO S, et al. A crucial role of angiotensin converting enzyme 2 (ACE2) in SARS coronavirus-induced lung injury. Nature Medicine, 2005, 11(8): 875–879.

[27] LI RQ, TIAN JG, YANG F, et al. The clinical study on the relationship between serum albumin concentration and lymphocyte levels in patients with 2019-novel coronavirus

pneumonia. Chinese Journal of Emergency Medicine, 2020, 29(4): 478–482.

[28] MALLICK B, GHOSH Z, CHAKRABARTI J. MicroRNome analysis unravels the molecular basis of SARS infection in bronchoalveolar stem cells. PloS One, 2009, 4(11): e7837.

[29] CHANNAPPANAVAR R, FEHR AR, VIJAY R, et al. Dysregulated type I interferon and inflammatory monocyte-macrophage responses cause lethal pneumonia in SARS-CoV-infected mice. Cell Host & Microbe, 2016, 19(2): 181–193.

[30] LI L, DAI B, LU F G, et al. Experimental study on Maxing Shigan Decoction with different proportions in treating mice infected with influenza virus. China Journal of Traditional Chinese Medicine and Pharmacy, 2017, 32(1): 309–313.

[31] WU YJ, FU XY, ZHANG XX, et al. Based on the principle of "three measures" to explore the differences of different traditional Chinese medicine schemes for new coronary pneumonia. Chinese Journal of Experimental Pharmacology, 2020: 1-8 [2020-05-08]. https://doi.org/10.13422/j.cnki.syfjx.20201326.

[32] HUANG C, WANG Y, LI X, et al. Clinical features of patients infected with 2019 novel coronavirus in Wuhan, China. The Lancet, 2020, 395(10223): 497–506.

[33] ZHANG YM, YU L, TANG LL, et al. A Promising Anti-Cytokine-Storm targeted therapy for COVID-19: The Artificial-Liver Blood-Purification System. Engineering (Beijing, China), 2020. https://doi.org/10.1016/j.eng.2020.03.006

[34] PHUA J, WENG L, LING L, et al. Intensive care management of coronavirus disease 2019 (COVID-19): challenges and recommendations. The Lancet Respiratory Medicine, 2020, 8(5): 506–517.

[35] CAO XT. COVID-19: immunopathology and its implications for therapy. Nature Reviews Immunology, 2020, 20: 269–270.

[36] XU XL, HAN MF, LI TT, et al. Effective treatment of severe COVID-19 patients with tocilizumab. Proceedings of the National Academy of Sciences of the United States of America, 2020, 117(20):10970-10975.

[37] LIU T, ZHANG JY, YANG YH, et al. The potential role of IL-6 in monitoring coronavirus disease 2019. MedRxiv, 2020.

[38] HEROLD T, JURINOVIC V, ARNREICH C, et al. Level of IL-6 predicts respiratory failure in hospitalized symptomatic COVID-19 patients. MedRxiv, 2020.

[39] LI RF, HOU YL, HUANG JC, et al. Lianhuaqingwen exerts anti-viral and anti-inflammatory activity against novel coronavirus (SARS-CoV-2). Pharmacological Research, 2020, 156: 104761.

[40] TAN L. Study of Maxingshigan Decoction on lung inflammation and lung TLR7/8 gene, protein expression level of mice infected by influenza A virus. Changsha: Hunan University of Chinese Medicine, 2014.

基于网络药理学的麻杏石甘汤干预新型冠状病毒肺炎作用机制探析

张世鹰[a, b, c], 李玲[a], 张宁[d, e], 夏洪涛[b, c], 卢芳国[a*], 李卫青[b, c*]

a. 湖南中医药大学, 湖南 长沙 410208, 中国
b. 深圳市罗湖区人民医院中医科, 广东 深圳 518001, 中国
c. 深圳大学第三附属医院中医科, 广东 深圳 518001, 中国
d. 深圳市罗湖区人民医院呼吸科, 广东 深圳 518001, 中国
e. 深圳大学第三附属医院呼吸科, 广东 深圳 518001, 中国

【摘要】目的 探析麻杏石甘汤(MXSGD)干预新型冠状病毒肺炎(COVID-19)的作用机制。**方法** 基于药代动力学参数通过 TCMSP 数据库、TCM Database@Taiwan 数据库筛选 MXSGD 的成药性活性成分及其调控的蛋白靶标,随后通过 String 数据库获得新型冠状病毒转染宿主的(COVID-19)ACE2 受体及与之相互作用的相关靶点,利用 Cytoscape 3.7.2 构建相关网络并进行网络拓扑学分析,对网络中的核心靶点通过 DAVID 数据库进行基因本体(GO)富集分析和信号通路富集分析。**结果** 共收集到 272 个 MXSGD 靶点和 21 个新型冠状病毒(SARS-CoV-2)肺炎的潜在靶点。在此基础上,构建并分析了 4 个网络:(1)MXSGD 成分-靶点网络;(2)MXSGD-SARS-CoV-2 蛋白质互作网络;(3)MXSGD-SARS-CoV-2 蛋白质互作网络子簇;(4)单味药-信号通路-靶点网络。其核心靶点为 AKT1、MAPK3、IL-6、TP53、VEGFA、TNF、CASP3、EGFR、EGF、MAPK1 等;GO 富集分析显示相关生物模块包括炎症反应(炎性细胞、炎性细胞因子及其信号转导途径)、免疫反应(T 细胞、单核细胞、B 细胞等免疫细胞)、免疫因子(IFN-γ、TNF-α 等)、病毒防御、体液免疫和黏膜固有免疫反应等;信号通路富集显示相关信号通路包括 TNF 信号通路、NOD 样受体信号通路、FoxO 信号通路、PI3K-AKT 信号通路、Toll 样受体信号通路等。**结论** MXSGD 可通过多组分、多靶点调控新型冠状病毒性肺炎;它可以通过调节与 ACE2 相互作用的几种蛋白质和一系列与疾病发展密切相关的信号通路来减轻炎症反应及调节免疫平衡。

【关键词】新型冠状病毒肺炎;麻杏石甘汤;网络药理学;作用机制;ACE2 受体